Annales Geophysicae (2003) 21: 457–472 © European Geosciences Union 2003

Annales Geophysicae

Evidence for impulsive solar wind plasma penetration through the dayside magnetopause

R. Lundin[1,2], J.-A. Sauvaud[1], H. Rème[1], A. Balogh[3], I. Dandouras[1], J. M. Bosqued[1], C. Carlson[4], G. K. Parks[4], E. Möbius[5], L. M. Kistler[5], B. Klecker[6], E. Amata[7], V. Formisano[7], M. Dunlop[3], L. Eliasson[2], A. Korth[8], B. Lavraud[1], and M. McCarthy[9]

[1]CESR, Toulouse, France
[2]Swedish Institute of Space Physics, Kiruna, Sweden
[3]Imperial College, London, UK
[4]Space Sciences Laboratory, University of California Berkeley, USA
[5]EOS, University of New Hampshire, Durham, NH, USA
[6]MPI für extraterrestrische Physik, Garching, Germany
[7]IFSI, Rome, Italy
[8]MPI für Aeronomie, Katlenburg-Lindau, Germany
[9]Space Program, University of Washington, USA

Received: 3 September 2001 – Revised: 25 March 2002 – Accepted: 20 June 2002

Abstract. This paper presents in-situ observational evidence from the Cluster Ion Spectrometer (CIS) on Cluster of injected solar wind "plasma clouds" protruding into the dayside high-latitude magnetopause. The plasma clouds, presumably injected by a transient process through the dayside magnetopause, show characteristics implying a generation mechanism denoted impulsive penetration (Lemaire and Roth, 1978).

The injected plasma clouds, hereafter termed "plasma transfer events", (PTEs), (Woch and Lundin, 1991), are temporal in nature and relatively limited in size. They are initially moving inward with a high velocity and a magnetic signature that makes them essentially indistinguishable from regular magnetosheath encounters. Once inside the magnetosphere, however, PTEs are more easily distinguished from magnetopause encounters. The PTEs may still be moving while embedded in an isotropic background of energetic trapped particles but, once inside the magnetosphere, they expand along magnetic field lines. However, they frequently have a significant transverse drift component as well. The drift is localised, thus constituting an excess momentum/motional emf generating electric fields and currents. The induced emf also acts locally, accelerating a pre-existing cold plasma (e.g. Sauvaud et al., 2001).

Observations of PTE-signatures range from "active" (strong transverse flow, magnetic turbulence, electric current, local plasma acceleration) to "evanescent" (weak flow, weak current signature).

PTEs appear to occur independently of Interplanetary Magnetic Field (IMF) B_z in the vicinity of the polar cusp region, which is consistent with observations of transient plasma injections observed with mid- and high-altitude satellites (e.g. Woch and Lundin, 1992; Stenuit et al., 2001). However the characteristics of PTEs in the magnetosphere boundary layer differ for southward and northward IMF. The Cluster data available up to now indicate that PTEs penetrate deeper into the magnetosphere for northward IMF than for southward IMF. This may or may not mark a difference in nature between PTEs observed for southward and northward IMF. Considering that flux transfer events (FTEs), (Russell and Elphic, 1979), are observed for southward IMF or when the IMF is oriented such that antiparallel merging may occur, it seems likely that PTEs observed for southward IMF are related to FTEs.

Key words. Magnetospheric physics (magnetopause, cusp, and boundary layers; magnetosphere-ionosphere interactions; solar-wind magnetosphere interactions)

Correspondence to: R. Lundin (rickard.lundin@irf.se)

1 Introduction

The entry of magnetosheath plasma through the dayside magnetopause and the associated transfer of energy into the magnetosphere remains a key problem in magnetospheric physics. The problem of energy, mass and momentum transfer from the solar wind is predominantly discussed in terms of reconnection near the subsolar region of the magnetosphere. Reconnection may not be restricted to the subsolar

region, in particular for northward IMF when reconnection is inferred to take place in the nightside/lobe region. Magnetic reconnection is by definition considering magnetic fields and convecting flux tubes attached to the solar wind flow in the momentum exchange process. From a plasma-kinetics point of view, however, it is unsatisfactory to consider fields and particles separately in an energy and momentum transfer process. No matter how tempting it may be to consider "ideal" conditions, such as "frozen in flux tubes", such oversimplifications may easily become misleading, in particular since observations tell us that the transfer of energy from the solar wind into the magnetosphere includes a number of key parameters: for example, the solar wind plasma dynamics, the magnetosphere plasma dynamics, the ionospheric plasma acceleration and outflow, the generation of magnetospheric currents and fields interconnecting dynamo and load regions are all embedded in ambient electric- and magnetic fields generated remotely but projecting onto the locus of observation. To distinguish cause from effect remains a challenge in contemporary space plasma physics.

An example of the aforementioned cause-effect difficulties can be illustrated by two categories of observations, flux transfer events, FTEs (e.g. Russell and Elphic, 1979) and magnetosheath plasma transfer events, PTEs (e.g. Carlson and Torbert, 1980; Lundin and Dubinin, 1985; Woch and Lundin, 1991). For instance, FTEs first detected by magnetometers are naturally linked not only to field-aligned currents (e.g. Russell, 1984) but also to the transfer of solar wind plasma into the magnetosphere. Conversely, PTEs relate from an observational point of view more to impulsive plasma penetration introduced by Lemaire and Roth (1978): i.e. plasma intrusions through the magnetopause may induce current signatures similar to those associated with FTEs (Lundin, 1989). The question remains what is cause and what is effect. Two causal aspects are of interest:

1. magnetic reconnection causes plasma transfer or plasma transfer leads to a magnetic x-line topology;

2. The ambient magnetic field frozen into the plasma (except at the x-line) gives the topology and provides the conditions for transfer or the topology and conditions for transfer are defined by the intrinsic properties of the plasma, inducing local perturbation fields and currents. These aspects require careful consideration on basis of observational data.

From a plasma physics point of view the magnetopause is associated with a multitude of physical processes that remain to be explored in much more detail. For instance, one may argue that plasma acceleration and deceleration in the magnetopause current sheet are as complex and variable as plasma acceleration on auroral field lines. In a similar way, the injection of plasma through the magnetopause may take place by a range of processes from weak diffusion to massive transient injection (from a minor wave induced leakage through an apparent pristine boundary) to a direct inflow through "holes" created by instabilities at the magnetopause boundary.

The history of impulsive penetration, i.e. transient solar wind plasma injection, dates back to the late seventies and early eighties. Lemaire and co-workers (Lemaire, 1977; Lemaire and Roth, 1978) proposed that elements of solar wind plasma may impulsively penetrate into Earth's magnetosphere as a consequence of solar wind irregularities and their intrinsic magnetization. Later Heikkila (1982) proposed that the impulsive penetration process may be governed by inductive electric fields set up at the magnetopause for favorable conditions. Owen and Cowley (1991) refuted Heikkila's model and argued that it does not work. Disregarding all the arguments, there has been a tendency to either distrust or simply ignore observational facts. Plasma does indeed penetrate the magnetopause and populates closed terrestrial magnetic field lines. Moreover, plasma elements "bulleting" across magnetic field lines were observed in the laboratory in the fifties (Bostik et al., 1956), and the theoretical grounds for such observations were subsequently established by Schmidt (1960).

As for the theoretical understanding, the early ideas by Lemaire and Heikkila were partly supported by theoretical arguments (e.g. Schindler, 1979) but only for exactly anti-parallel magnetic fields at the magnetopause. Simulations later demonstrated (e.g. Ma et al., 1991) that the anti-parallel conditions may be softened to within about five degrees. A theoretical recognition of observational facts is therefore slowly emerging. However, as will be demonstrated here, and as has been reported previously (e.g. Woch and Lundin, 1992; Stenuit et al., 2001), a strict magnetic boundary condition set up by the IMF and the magnetospheric low-latitude B-field does not correspond sufficiently well to experimental data on the access of plasma through the magnetopause. We are obviously still at a state where observations lead the efforts to adequately understand the physics of solar wind energy, mass and momentum transfer through the magnetopause.

In this report we focus on ion observations from the Cluster CIS characteristic of plasma transfer events, i.e. observations of magnetosheath plasma structures penetrated into the magnetosphere. The cases selected here are less ambiguous from the point of view of separating magnetopause encounters from PTEs. The events represent "blobs" of streaming magnetosheath plasma embedded in magnetospheric plasma, injections that may protrude deep into the magnetosphere on closed magnetic field lines.

It is of particular interest to note that PTEs are associated with plasma acceleration, i.e. local/cold plasma taking up energy and momentum from the intruding plasma elements. The plasma acceleration is in agreement with what is expected from a polarisation electric field set up by the plasma motion transverse to the local magnetic field (e.g. Livesey and Pritchett, 1989; Lemaire and Roth, 1978; Lundin and Dubinin, 1985), i.e. the ions are accelerated transverse to the magnetic field. Frequent PTEs associated with local/cold plasma acceleration may become an important source of magnetospheric plasma as described by Sauvaud et al. (2001).

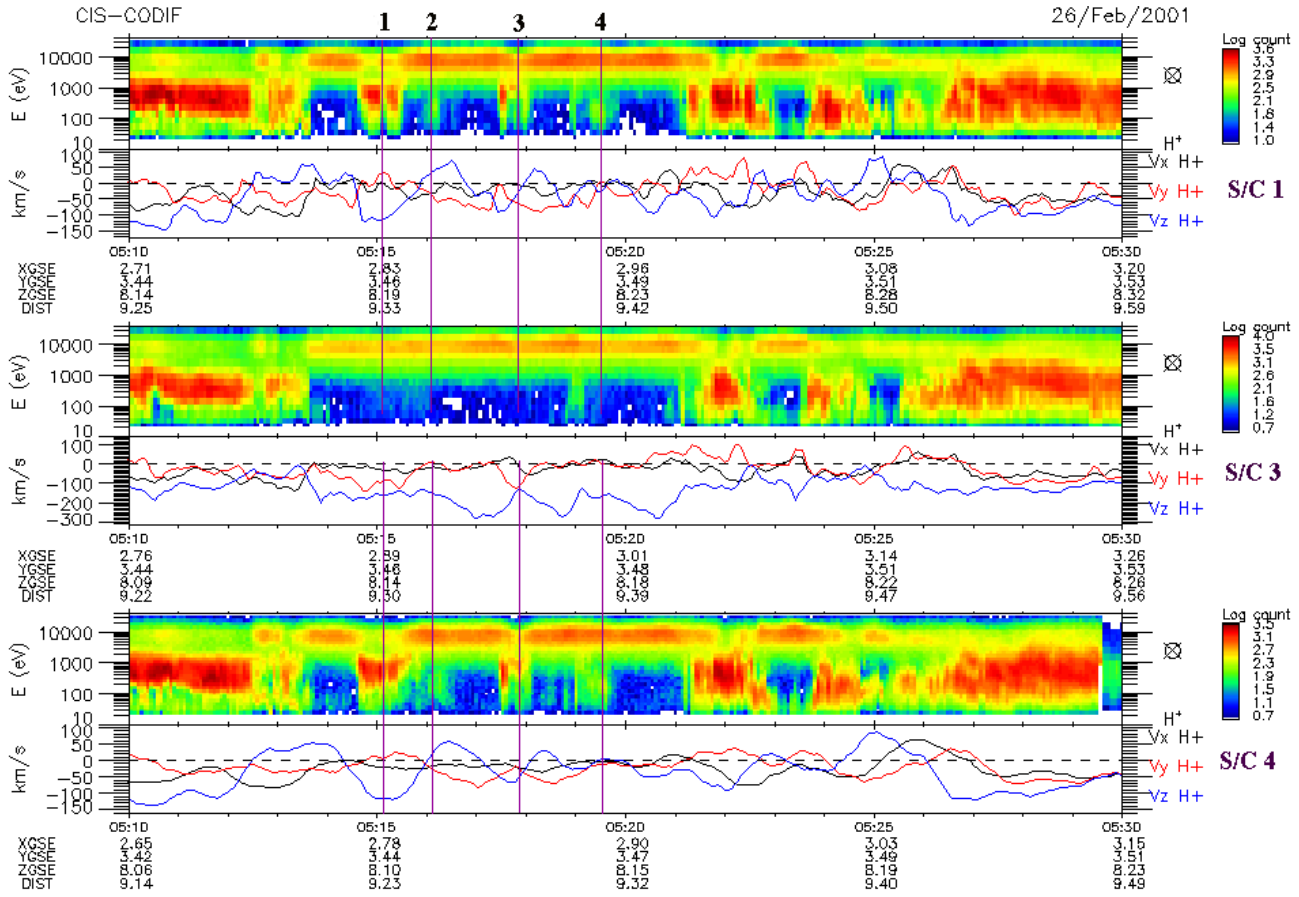

Fig. 1. Cluster CIS data from 26 February 2001, displaying a series of magnetosheath plasma transfer events (marked by **(1)**, **(2)**, **(3)** and **(4)**), embedded in a background of more energetic ring current/plasma sheet plasma (≈05:14–05:21 UT). The data were taken during a time when the IMF B_z was ≈0 nT and the IMF B_y was ≈−1 nT.

2 Observations

The particle data come from the Cluster Ion Spectrometer (CIS) experiment (Rème et al., 2001), comprising two instruments:

1. a Hot Ion Analyser, CIS-2, measuring the ion distribution from 5 eV to 26 keV using a classical symmetrical quadrispherical analyser and a fast particle imaging system based on micro-channel plate electron multipliers and position-encoding discrete anodes;

2. a time-of-flight mass spectrometer, CIS-1, which combines a top-hat analyser with an instantaneous 360°×8° field of view with a time of flight section to measure complete 3-D distribution functions of the major ion species. Typically these include H^+, He^{++}, He^+ and O^+. The sensor primarily covers the energy range between 0.02 and 38 keV/q.

The magnetic field data come from the fluxgate magnetometers (FGM) installed on board the Cluster spacecraft (Balogh et al., 1997). These data are averaged over 4 s. An instrument for active spacecraft potential control (ASPOC) is used to lower the satellite potential by emitting a current of Indium ions (Riedler et al., 1997).

Figure 1 shows CIS data from 26 February 2001, displaying a series of magnetosheath plasma injection regions (marked 1, 2, 3 and 4) embedded in a background of more energetic ring current/plasma sheet plasma (≈05:14–05:21 UT). The four Cluster s/c passed first the cusp, then the boundary layer/dayside outer ring current (BL/RC), finally encountering briefly the magnetosheath (MS) at approximately 05:32–05:40 UT (not shown in Fig. 1). The data were taken during a time when the IMF, as determined from ACE data, was $B_z \approx 0$ nT and $B_y \approx -1$ nT. Well inside the magnetosheath, after ≈06.02 UT, the magnetic field B_x component measured by Cluster varied between ≈0 and 20 nT with quasiperiodic oscillations in the minute range, B_y and B_z being negative and also quite variable.

The panels are sectioned in three groups for s/c 1, s/c 3, and s/c 4, the three Cluster s/c with CIS data. The two panels in each section display energy-time spectrograms of ions and H^+ flow velocity in GSE co-ordinates. The PTEs, marked out by arrows and the digits 1, 2, 3 and 4, are characterised by regions of magnetosheath-like plasma imbedded in more energetic magnetospheric plasma. The "mixing" of

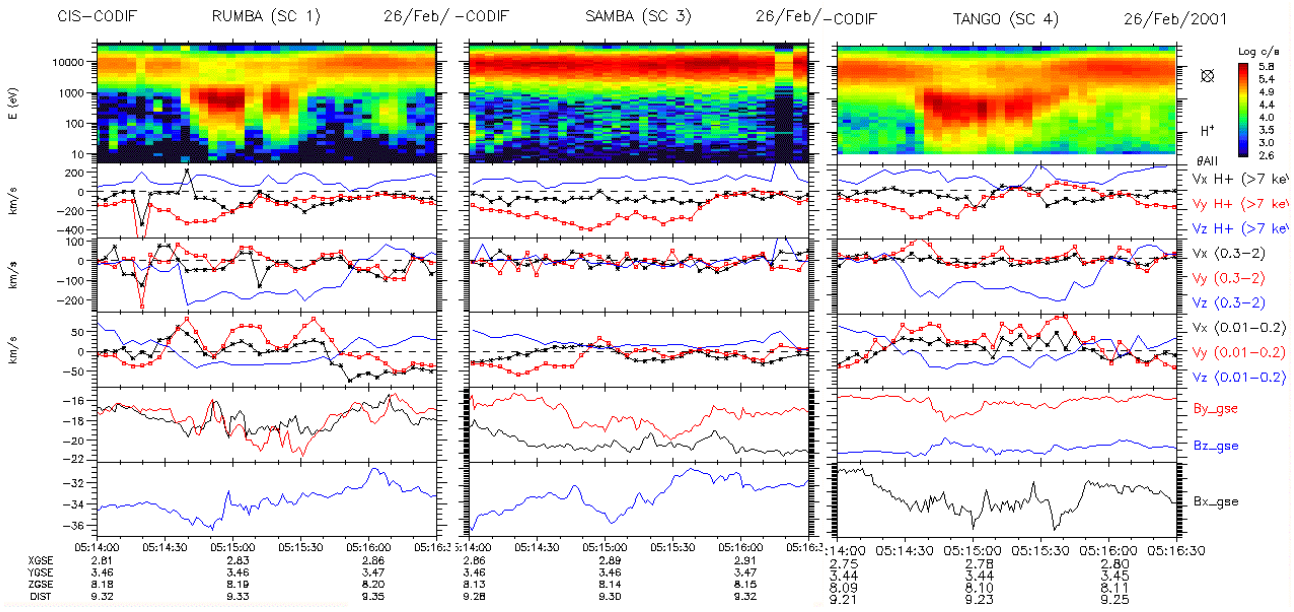

Fig. 2. A close-up view of one of the PTEs shown in Fig. 1 (26 February 2001) for the three s/c 1, 3 and 4. Upper panels give the energy-time spectrum of ions, panels 2 the flow velocity for >7 keV H^+, panels 3 the flow velocity for 0.3–5 keV H^+, panels 4 the flow for <0.2 keV H^+ and the bottom two panels the magnetic field components in GSE co-ordinates.

magnetosheath and magnetosphere ions within PTEs varies from full mixing (2, 4) to weak mixing (1, 3). Full mixing means that magnetosheath plasma is contained in magnetospheric plasma on apparently closed magnetic field lines (2, 4 in Fig. 1). Weak mixing marks a transition region – with magnetosheath plasma newly injected into magnetospheric plasma. The latter is associated with decreased fluxes of magnetospheric plasma on either open or closed magnetic field lines. Comparing the data from the three s/c, it is apparent that the PTEs vary with space and time. Notice, for instance that PTEs 1, 2 and 3 are not observed on s/c 3. The main spatial parameter explaining the void of PTEs, for s/c 3 during the time period 05:14–05:21 UT, is the distance in the solar direction (X), s/c 3 being some 0.05 Re (≈300 km) further sunward than s/c 1 and s/c 4. The observation is consistent with "embedded" plasma streaming downward close to the magnetic field direction, with s/c 3 outside it on magnetospheric field lines closer to the dayside magnetopause. We return to this issue later in our analysis.

The observations in Fig. 1 take place well inside the magnetopause on what appears to be open (cusp) and partly closed (BL/RC) magnetic field lines. By partly closed, we mean that the open-closed issue can only be resolved by considering the distribution of very energetic electrons which may not be available.

In what follows, we describe four cases of PTEs for solar wind IMF conditions varying from negative B_z to positive B_z, from newly injected events to old/evanescent PTEs.

Figure 2 gives a close-up view of PTE #1 in Fig. 1, again for the three s/c 1, 3, and 4. The top panels give energy-time spectrogram plots for ions using the CIS-2 (without mass selection) for s/c 1 and s/c 3 and using CIS-1 (H^+) for s/c 4. The PTE, observed on s/c 1 and s/c 4, is characterised by magnetosheath plasma embedded in a background of more energetic ions of plasmasheet/ring current origin. The event may be characterised by on-going mixing of two plasma populations in a limited region of space. The physics of the plasma mixing are of interest here.

The three panels, Figs. 2a–c, are each subdivided into six panels. The five lowermost panels show from the top the velocity deduced for ions greater than 7 keV, then the velocity calculated for 0.3–2 keV ions (solar wind regime), then the velocity for ions less than 0.2 keV, all velocity components given in GSE co-ordinates. The two lowermost panels give the three magnetic field components in GSE co-ordinates. The reason for the division into three energy ranges for the velocity computation is the identification of three separate ion components:

1. An ion component of plasma sheet origin (> 7 keV),
2. an injected magnetosheath component (0.3–2 keV) and
3. a "cold" plasma component that becomes visible under the effect of an enhanced electric drift in the boundary layer (<0.2 keV for H^+).

The three H^+ flow components may in fact display quite different characteristics, in particular during PTEs. The departure in flow direction for the three energy ranges represents the degree of inhomogeneity of the media. The lack of flow directionality differences within the three energy ranges implies homogeneity.

An example of a relatively similar flow behaviour of the three H^+ veolcity components is shown in Fig. 2b (s/c 3).

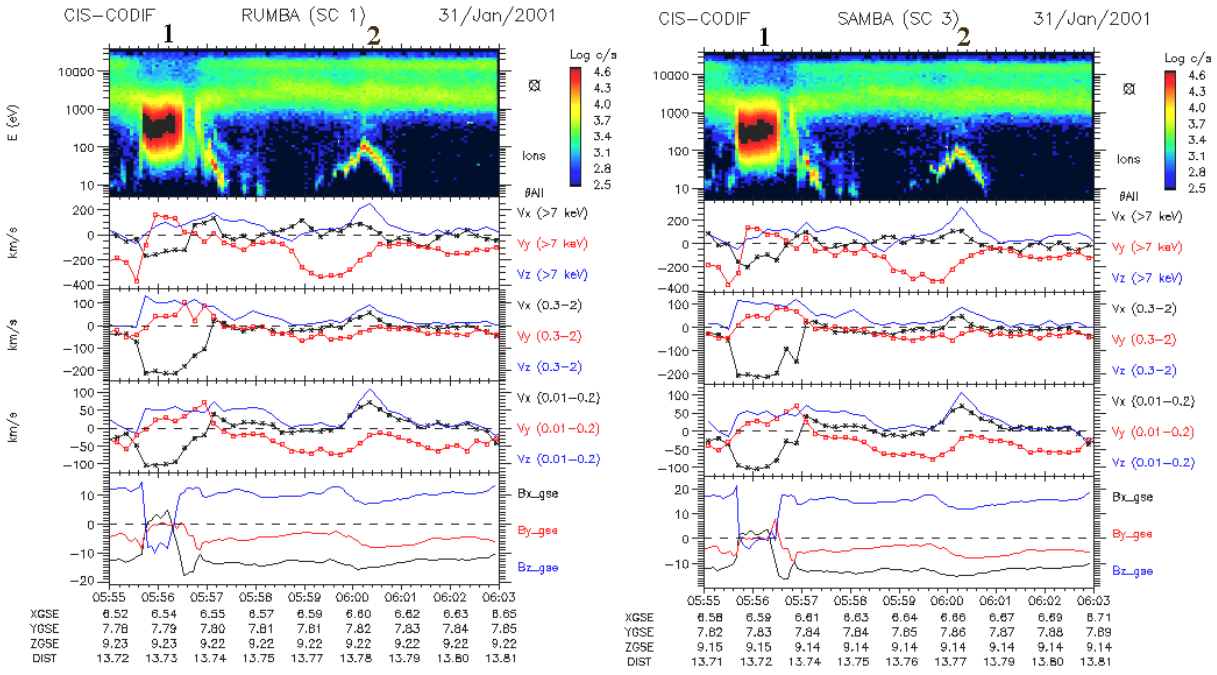

Fig. 3. Encounter of magnetosheath-like plasma on 31 January 2001, when the IMF was directed southward (−2 nT). This encounter is also described by Sauvaud et al. (2001). The first event (1) is dominated by magnetosheath plasma while the second (2) lacks such a signature.

Notice that the overall flow direction remains relatively uniform throughout this time interval in Fig. 2b, while there is a difference in flow magnitude. This difference in magnitude is mainly caused by the computational method, integrating the moments of the distribution function over different energy intervals. Since the average velocity is determined by $v = 1/n \int v \cdot f(v) dv$, where n is the number density, the cut in energy towards lower energies gives a systematically lower number density and consequently a systematically higher velocity for the high energy intervals.

The rather uniform flow of s/c 3 contrasts to the variable flow signatures of the PTEs observed by s/c 1 and s/c 4. While the ions of solar wind origin (0.3–2 keV) are flowing strongly in the -Z direction (in the PTE inward with respect to the Northern Hemisphere) the energetic ions (>7 keV) display an apparent flow in the opposite direction. However, the energetic ion "flow" is most likely the effect of a plasma pressure gradient, perpendicular as well as along the magnetic field direction. In fact, velocities obtained from moment computations cannot distinguish spatial/temporal gradients from bulk flows. Higher order moments are required for that distinction. But for our purposes here it is sufficient to note that any difference in component flows is most likely associated with gradients in the plasma. Notice, for instance, the deviation of the >7 keV V_y-component preceding the PTE encounter for s/c 1 and s/c 4. Because B_z is a strong magnetic field component, one may qualitatively regard the V_x and V_y components as representing transverse pressure gradients. Indeed, the characteristics of the PTE are those of a depletion of energetic ions, a region that can be "remotely sensed" by the more energetic ions with large Larmor radii. This then explains the similar negative excursion of the >7 keV $V_y$component for s/c 3; i.e. although not directly encountering the PTE, it can be remotely sensed by energetic ions from s/c 3. The fact that the PTEs can be remotely sensed by s/c 3 implies that they are within a distance of two Larmor radii of >7 keV protons.

The low-energy ions (<0.2 keV) are of particular interest because due to their small ion Larmor radii the drift perpendicular to B should be dominated by the electric drift. We return to the electric drift later in the analysis but, for the time being, we merely note some important ion drift properties within the PTE. From Fig. 2, we see that the mid-energy (0.3–2 keV) and low energy (<0.2 keV) ion flow is rather similar, i.e. the Z-component dominates. Some deviation may be observed, e.g. in magnitude and preceding and succeeding the event, but the overall tendency is the same. The main difference is in the magnitude of the flow velocity. A first reaction is to simply discard this as being due to moments computed for separate energies, leading to higher velocities for intervals with higher energies. However, as will soon become apparent, the two populations may indeed drift with different velocities. In this case, the injected sheath plasma is drifting with 250–350 km/s while the low-energy ions drift with velocities 100–200 km/s, i.e. about half the drift velocity of the more energetic population. From this we can conclude that the transverse drift of ions is not only due to an electric drift, one must also consider other drift terms as discussed by Lundin et al. (1987).

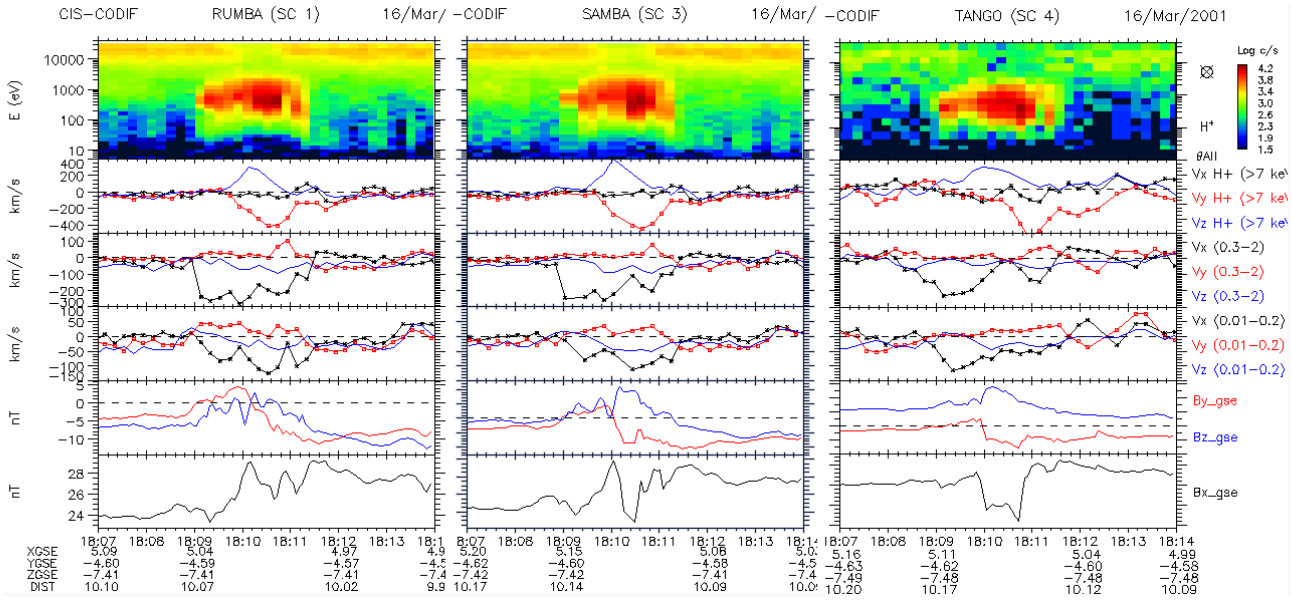

Fig. 4. A PTE from 16 March 2001, observed well inside the magnetosphere and apparently embedded in plasma sheet/ring current plasma. The injected magnetosheath ions (0.3–2 keV) are still streaming essentially anti-sunward with a velocity of about 200 km/s while the background plasma is either streaming only moderately or just responding to the plasma gradient (>7 keV). IMF: $B_z \approx 1$ nT, $B_y \approx 4$ nT.

Figure 3 shows the encounter of magnetosheath-like plasma on 31 January 2001, when the IMF was directed southward (−2 nT). This encounter is also described by Sauvaud et al. (2001). The first event (1) is dominated by magnetosheath plasma, while the second (2) lacks such a signature.

The two lowermost panels of Fig. 2, showing the FGM magnetic field data, indicate that this PTE was associated with a magnetic perturbation of up to 30% of the B_y and B_z components. A relatively weak total pressure increase (not shown here) was also associated with this PTE.

Figure 3 represents a case of potential PTEs when the IMF was directed southward (−2 nT). In this case, however, it was not clear whether the magnetosheath plasma event represents a plasma intrusion. An alternative, perhaps even more likely, interpretation is a magnetopause encounter, the magnetopause moving in and out and crossing the satellites. Nevertheless, the nature of this encounter, also described by Sauvaud et al. (2001), is interesting. The two events displayed in Fig. 3 occur at ≈05:56 UT and ≈06:00 UT, respectively. Both events are associated with an adiabatic "acceleration" of cold ions in a layer with enhanced electric drift immediately inside the magnetopause as discussed by Sauvaud et al. (2001). We notice that, as in Fig. 2, the overall flow characteristics of the "solar wind" (0.3–2 keV) and "cold" (<0.2 keV) ions is similar inside the injection structure, albeit with a different V_x flow velocity. Thus, it seems as if the latter two ion populations track each other within the injection structure but with differences in the magnitude of the velocity, especially in the X-direction. The major difference is that the "cold" ions display another flow characteristic that is due to a varying electric field within the boundary layer. The overall similarity in all three energy passbands during the remaining time interval of Fig. 3 is indicative of a predominant electric drift.

A further aspect of Fig. 3 is the magnetic perturbation in the region of enhanced cold ion drift, i.e. on the magnetospheric side of the magnetopause, 2. The bipolar perturbation of B from the mean for all three components may be interpreted as the traversal of a field-aligned current flux tube, similar to flux transfer events (FTEs). The ≈5 nT perturbation of the Y- and Z-components corresponds to a downward current of $\approx 10^{-7}$ A/m^2. Notice that a similar magnetic perturbation can also be found at the innermost boundary of the injection signature, 1. The PTEs in Fig. 3 were observed near the magnetopause for southward IMF which suggests that they are synonymous with FTEs (e.g. Russell and Elphic, 1979). A more careful analysis of the magnetic field data is required to resolve this issue, however.

Figure 4 illustrates a PTE located well inside the magnetosphere, i.e. apparently embedded in the plasma sheet/ring current plasma. Notice, however, that the injected magnetosheath ions are still streaming anti-sunward with a velocity of about 200 km/s although with quite variable characteristics for different s/c. The energetic ion (>7 keV) flow structure illustrates the anisotropy related to the reduced flux of energetic ions inside a PTE. Using the energetic ion remote sensing technique, we may infer from the >7 keV "flow" that the central portion of the PTE (the reduction of energetic ion fluxes) was located in the -Y and +Z direction with respect to s/c 1 and 3. In the case of s/c 4, the count-rate is lower, due to a low-sensititivity mode, and the >7 keV "flow" signature indicates that the structure is oriented in the +Z direction. This is in good agreement with the GSE location of the three s/c

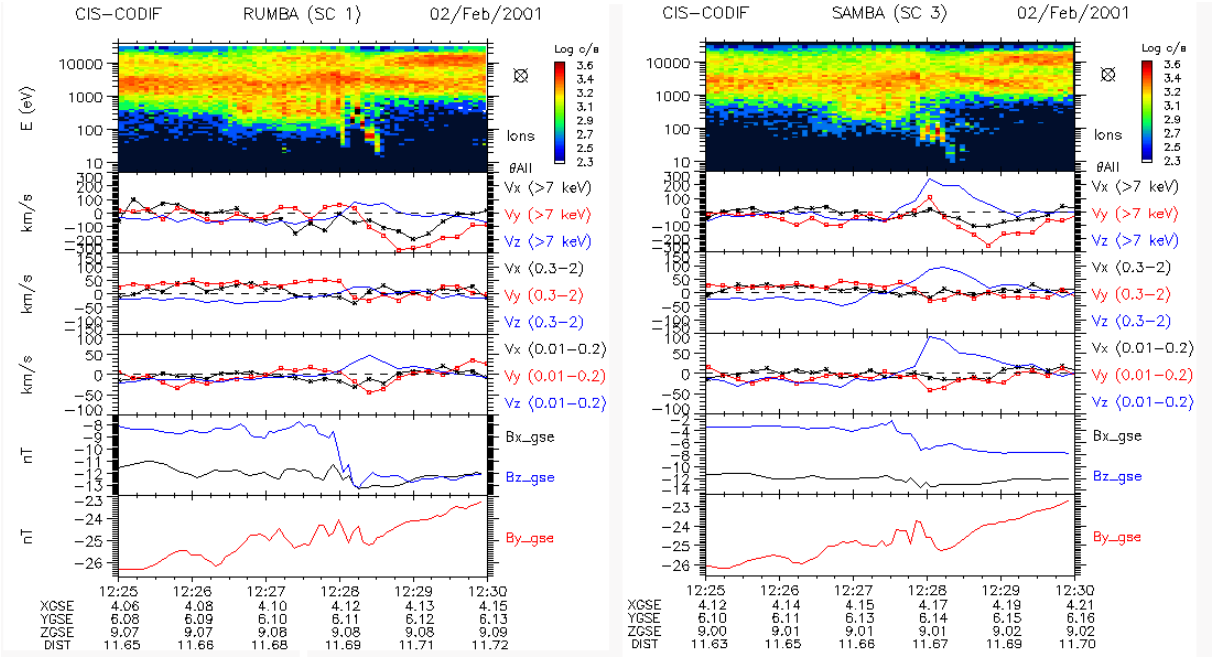

Fig. 5. A PTE (2 February 2001) with fully "mixed" plasma. No anti-sunward flow is observed in this PTE, indicating that the structure is stagnant yet with signs of activity as evidenced by the electric drift at the boundary and the field-aligned current signature (see text). The IMF: $B_z \approx 3$ nT, $B_y \approx 0$ nT.

provided that the PTE structure is drifting in the -Y and -Z direction, i.e. essentially away from the Earth in the YZ-plane but with an essentially anti-sunward plasma flow.

Our final example of a PTE, Fig. 5, represents a case when the three plasma components have been well "mixed". Only weak flow, attributed to electric drift, is observed in this PTE, indicating stagnation and evanescence. The lack of typical magnetosheath plasma characteristics (e.g. strong plasma flow) makes the identification of evanescent PTEs more difficult. However, this case is characterised not only by a "mid-energy" ion population but also by accelerated cold ions with a signature very similar to the PTE in Fig. 3. This PTE is still associated with some energy release as evidenced by a flow in the +Z direction attributed to an electric drift, the drift corresponding to an inward directed electric field by up to 3 mV/m. Notice that all three energy intervals display a similar directional flow, essentially perpendicular to B, implying that the electric drift is dominating here. Immediately adjacent to or preceding the electric drift region is a magnetic perturbation marking a ≈5 nT decrease of the Z-component, the other two magnetic field components remaining essentially unchanged. This is the characteristic of the traversal of an extended (in the XY-plane) current sheet. The properties of this PTE suggest that the satellites traversed a field-aligned current sheet with the current vector pointing upward, i.e. antiparallel with the magnetic field. Furthermore, the current sheet is associated with a converging electric field. An obvious interpretation is that the upward current is driven by a magnetospheric dynamo process, as discussed in the next section (Fig. 9).

Table 1. Plasma Transfer Events detected by Cluster CIS

Date	Time	B_x	B_y	B_z	No. of PTEs
26 Jan 2001	08:30–09:20	2	2	-5	15
31 Jan 2001	05:15–06:15	5	0	-1	7
2 Feb 2001	12:00–14:30	-1	-1	2	15
16 Feb 2001	19:15–20:00	2	-2	2	12
19 Feb 2001	02:30–03:30	0	-4	0	6
21 Feb 2001	11:00–12:15	7	-1	0	10
26 Feb 2001	05:15–05:45	-2	-1		5
10 Mar 2001	14:00–04:45	-2	2	-1	8
14 Mar 2001	22:30–23:00	2	-4	1	5
15 Mar 2001	00:00–01:00	-1	3	0	8
16 Mar 2001	17:15–19:00	-2	4	-5-+2	14
17 Mar 2001	06:45–09:15	-1	2	4	9
22 Mar 2001	01:00–02:45	-1	7	2	20
					134

The present study is based on the analysis of three months of Cluster dayside magnetopause crossings, focusing on 29 specific crossings from January to March 2001. Because the satellite passes over a limited portion of the dayside magnetosphere, much further analysis and more data on other parts of the magnetopause is required to complete the pic-

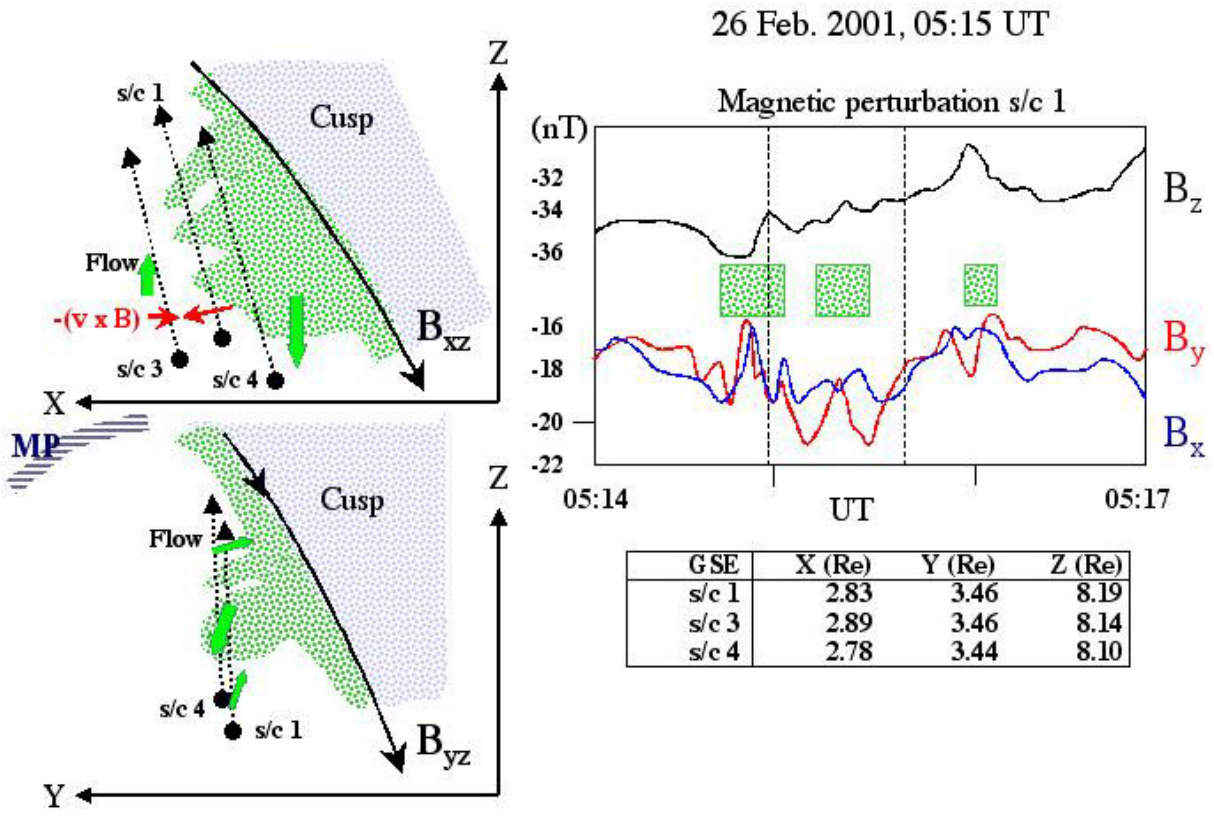

GSE	X (Re)	Y (Re)	Z (Re)
s/c 1	2.83	3.46	8.19
s/c 3	2.89	3.46	8.14
s/c 4	2.78	3.44	8.10

Fig. 6. Diagrammatic representation of several PTEs located immediately equatorward of the cusp as observed by Cluster s/c 1, 3 and 4 on 26 February 2001, 05:14–05:17 UT.

Table 2. Summary of PTEs for different IMF conditions

IMF B_x	<0	≈ 0	>0
No. of PTEs	79	6	49
IMF B_y	<0	≈ 0	>0
No. of PTEs	53	7	74
IMF B_z	<0	≈ 0	>0
No. of PTEs	30	36	63

ture. However, to illustrate the number of observations made in the present study we provide in Table 1 and Table 2 preliminary statistics from 13 of the 25 crossings when PTEs were clearly identified. Notice that the PTE identification was conditioned to regions that were identified as ring current/plasma sheet, excluding all cases clearly associated with open field lines such as in the cusp. Besides summarising the data base and listing the number of PTEs identified for different orbits, Table 1 also summarises the related solar wind conditions. On the basis of this we note that most of the PTEs are found for $B_z > 0$, but several cases are also found for $B_z < 0$. On the other hand there does not appear to be any significant IMF B_x or IMF By dependence on the occurrence of PTEs. Table 2 summarises the number of PTEs found for different IMF conditions.

3 Plasma motion, fields and currents in PTEs

The plasma properties observed for PTEs, and their association with physical processes, were discussed in very general terms in relation to Figs. 1–5. An obvious next step is to investigate the spatial/temporal characteristics and the local electromagnetic impact of PTEs. How localised are PTEs? What are their motional characteristics? And how do PTEs connect to the ambient magnetospheric plasma environment? The advent of the Cluster satellites, to probe the plasma structure in three dimensions, helps us to address these issues. Our first approach to reveal the three-dimensional properties of PTEs, is illustrated in Fig. 6. Figure 6 gives a diagrammatic representation of the PTE traversals in Fig. 2. The left side of Fig. 6 illustrates the PTE traversals as conceived in the XZ- and YZplanes (GSE) respectively. The right side is a diagram with magnetic field data (FGM) from s/c 1, illustrating the relatively complex magnetic perturbation associated with the PTE encounters of s/c 1 during this time period. Notice that the PTEs during this time interval are located adjacent to the cusp, the cusp traversal taking place prior to this between ≈04:00–05:00 UT. The PTE shape may be different from that of Fig. 6 but the structure is appar-

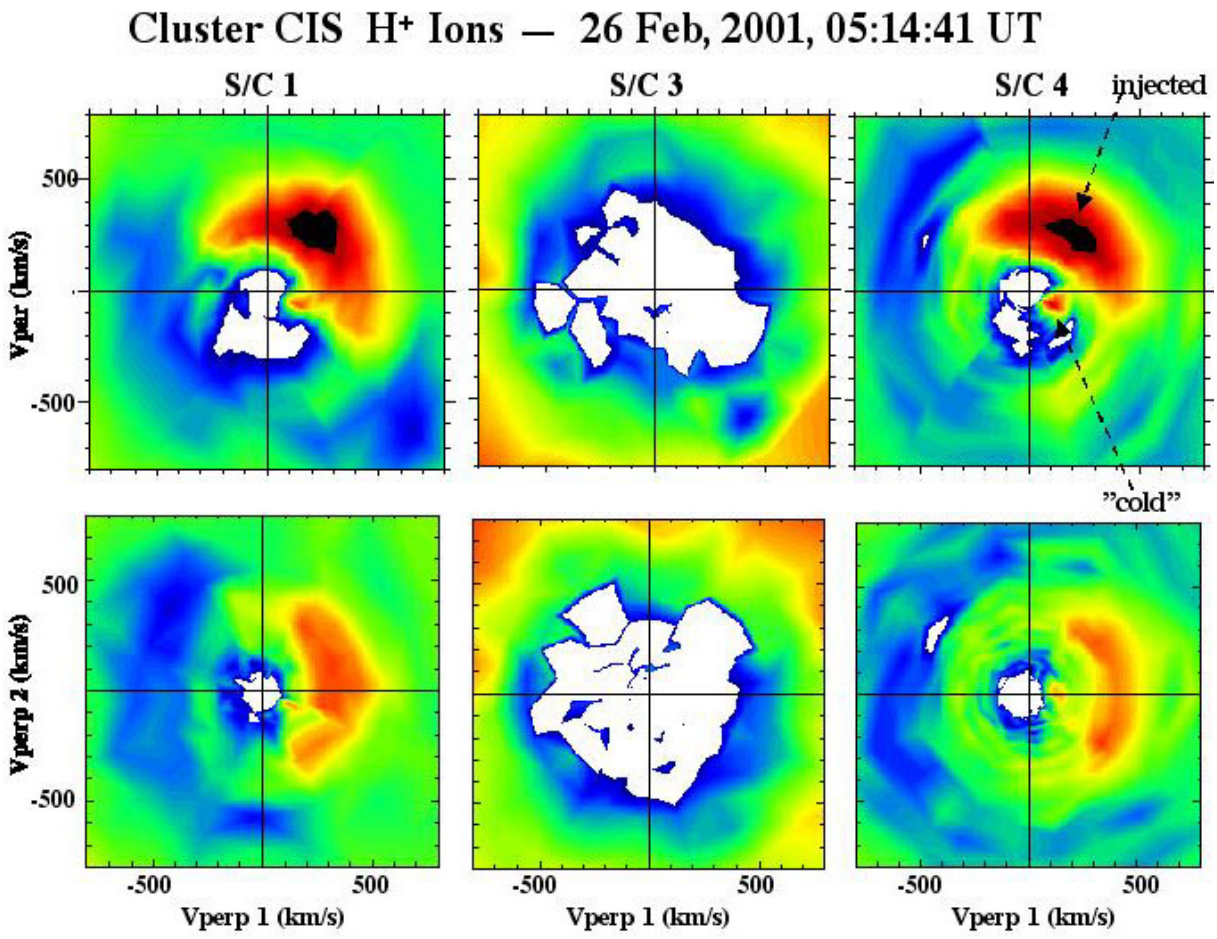

Fig. 7. H^+ velocity distribution, parallel and perpendicular to the magnetic field, for the PTE on 26 February 2001 described in Fig. 2. Notice the difference in transverse velocity for the injected magnetosheath plasma and the local "cold" plasma.

ently "embedded" in the magnetosphere, most likely with a dominating extension along the field line within a region of quasi-trapped energetic ions. However, PTEs are not only expanding along the magnetic field lines. The bulk flow (broad arrows) and the magnetic field orientation show that there is a strong transverse drift/convection motion of the plasma. The strong drift motion is more clearly demonstrated by Fig. 7, which gives a velocity contour plot of H^+ ions in magnetic field co-ordinates (velocity parallel and perpendicular to the magnetic field). Notice the strong transverse drift component of the injected solar wind plasma associated with a transversely drifting/convecting "cold" H^+ ion component. Figure 7 clearly demonstrates that there is a marked difference in drift velocity for the solar wind ions and the "cold" H^+ ions, a difference that may be as high as 100 km/s. Such differences were first discussed in terms of a dynamo process where the injected solar wind plasma acts as a dynamo (an electromotive force, emf) and the local "cold" plasma acts as a load (see e.g. Lundin and Dubinin, 1985). The physics of the differential ion drift and its relation to the intrinsic properties of the plasma were also discussed later by Lundin et al. (1987), and Stasiewicz (1991). It is interesting to note the very strong similarity between the CIS data in Fig. 7 and the Prognoz-7 data from the 1980s (e.g. Fig. 2 by Lundin et al., 1987). By subtracting individual drift velocity vectors for different plasma populations one eliminates the electric drift term (that is independent of charge and mass). The remainder is a differential drift (Lundin et al., 1987) that relates to three terms: Pressure gradient drift (∇p), anisotropy drift (a) and inertia drift (i), given by the equation:

$$\boldsymbol{\Delta v}_\perp = (\boldsymbol{\Delta v})_{\nabla \mathrm{P}} + (\boldsymbol{\Delta v})_{\mathrm{a}} + (\boldsymbol{\Delta v})_{\mathrm{i}} \quad (1)$$

Under the assumption that "cold" ions drift primarily as a result of the electric drift we may infer, from Fig. 7, that there is a differential drift of about 100 km/s caused by a combination of pressure gradient, anisotropy and inertia drift. Whatever the cause, it is likely to be related to the quite variable magnetic perturbation observed in Fig. 6 for s/c 1, a perturbation that varies strongly with time and space as can be seen in Fig. 2.

The motional force of the injected magnetosheath plasma, specifically the transverse drift, represents a source of free energy – a motional *emf*. The motional *emf* is a source of electromagnetic energy that may again convert to kinetic en-

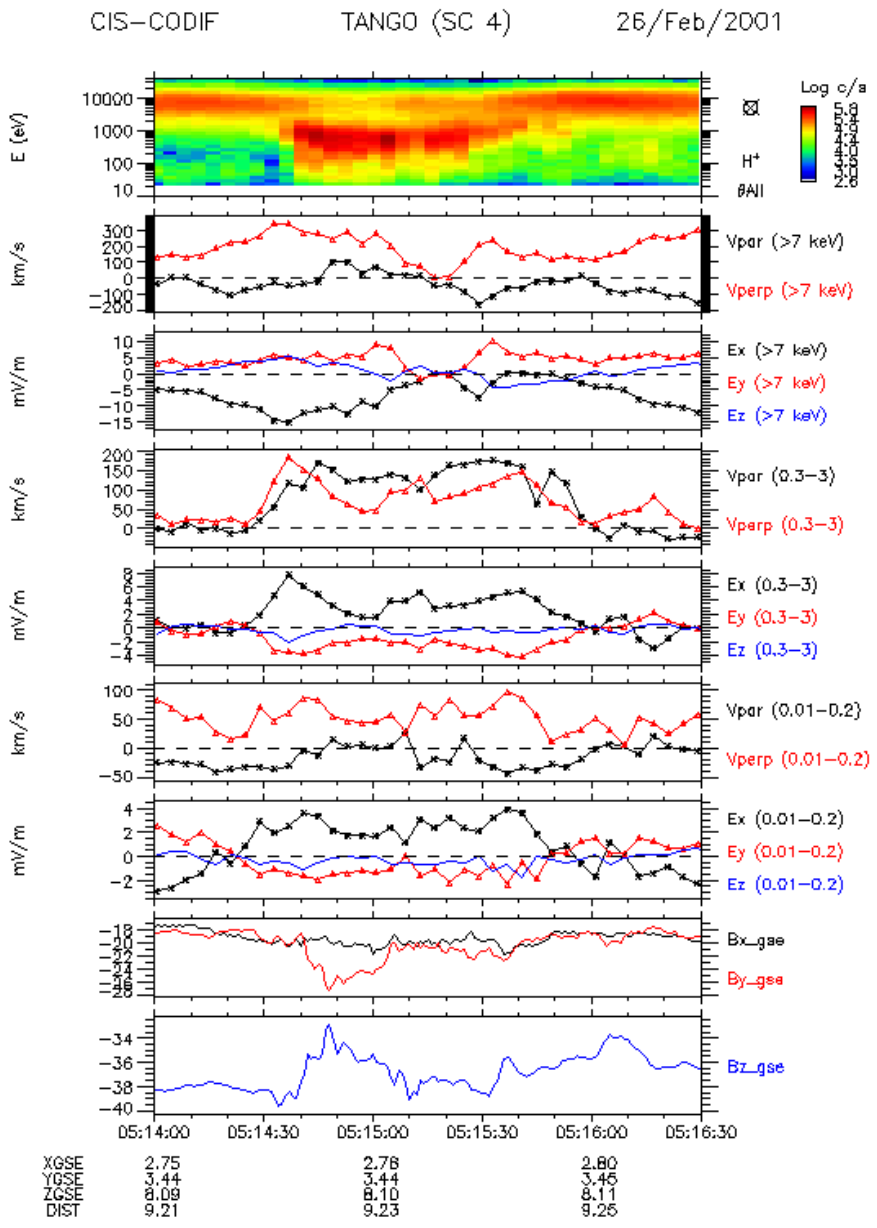

Fig. 8. H^+ parallel and perpendicular (to B) flow velocities and ($\boldsymbol{v} \times \boldsymbol{B}$) computed for three energy ranges (same as in Fig. 2–Fig. 5), for the PTE encountered during 26 February 2001.

ergy, accelerating and causing the drift of "cold" plasma (e.g. Fig. 7). It is, therefore, of interest to investigate the directional dependence of the *emf* (E) determined by the injected plasma flow, i.e.

$$\boldsymbol{E} = (\boldsymbol{v}_{\mathrm{inj}} \times \boldsymbol{B}) \qquad (2)$$

From the velocity and magnetic field components for s/c 1 and s/c 3 at 05:15 UT on 26 February 2001 we deduce the following vectors for the motional *emf* from the injected plasma flow (0.3–3 keV):

$\boldsymbol{E}$ = (4.7, -3, -0.5) mV/m for s/c 1 and

$\boldsymbol{E}$ = (-1.2, 1.2, 0) mV/m for s/c 3.

The *emf* vectors, also marked out in Fig. 6, illustrate the shear motion that exists in the region separating the plasma injection and its surroundings, the boundary indicating a region of negative polarity (converging electric field). The region of shear flow/converging electric field is related to currents, specifically field-aligned currents. The direction of the current is towards the region of negative charge, i.e. here antiparallel with the magnetic field direction (see Fig. 6). This corresponds to an upward field-aligned current connected to the ionosphere.

Figure 8 gives data from s/c 4 during the 26 February event, but now showing the parallel and perpendicular velocities and the *emf*(E) determined from the perpendicular flow (Eq. 2). Again, moments are computed for the above-mentioned three energy ranges. In addition to a clear difference in flow velocities, the data illustrate a difference in *emf*-terms between high energy- and mid/low energy-ions. This emphasizes again the need to separate ion species be-

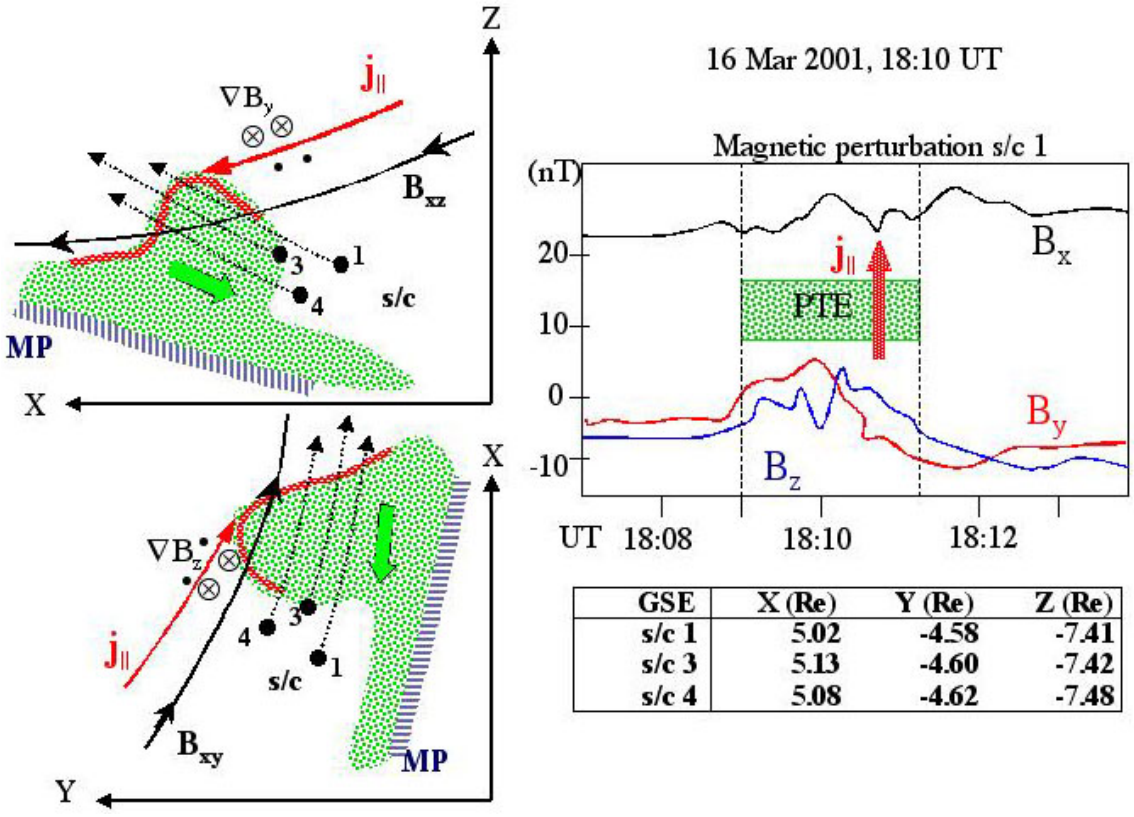

GSE	X (Re)	Y (Re)	Z (Re)
s/c 1	5.02	-4.58	-7.41
s/c 3	5.13	-4.60	-7.42
s/c 4	5.08	-4.62	-7.48

Fig. 9. Diagrammatic representation of the PTE on 16 March 2001, 18:10 UT.

fore plasma moments become useful quantities. Indeed, even the separation between mid- and low-energy ions is difficult in this case, the flow of the injected mid-energy ions dominating the appearance of the central time domain in the diagram. Outside this domain "cold" ions clearly show other flow characteristics compared to the injected mid-energy ions. Notice, though, the marked difference in flow characteristic between the injected and "cold" ions, the injected ions containing a significant field-aligned component while the "cold" ions are mainly drifting perpendicular to B.

Ampère's equation, $\nabla \times \boldsymbol{B} = \mu_o \boldsymbol{J}$, provides a more reliable way of determining the electric current discussed in conection with Fig. 6. The event on 16 March 2001 (Fig. 4) is, because of its relatively simple magnetic field characteristics, suitable for such an analysis. Figure 9 illustrates a PTE traversed by all three Cluster s/c on 16 March 2001. A PTE crossed the trajectory of the three s/c approximately positioned as illustrated in Fig. 9. Because of the high velocity of the PTE, the times of arrival were almost simultaneous yet the characteristics of the density and flow velocity varied considerably between the three s/c, obviously due to spatial inhomogeneities in the few hundred km range. Similar variations are also observed in the magnetometer data. Superimposed on the small-scale variations within PTEs, there is frequently a bimodal signature of B centered on the sunward side as displayed in Fig. 9. Based on the rotation of B, we have estimated the field-aligned current magnitude and direction which, for the case of Fig. 9 (and Fig. 4) is parallel/upward with a magnitude of $1 - 3 \cdot 10^{-7}$ (A/cm^{-2}). To determine the exact topology of the current structure with respect to the PTE requires a more thorough analysis of magnetic field data from all four Cluster s/c. A preliminary analysis shows that the currents are connected to the zone of strongest shear, which for a majority of the cases is on the sunward side of the PTEs.

Figure 10, representing the evanescent PTE on 2 February 2001 marginally modified by a flow in the XY-direction, enables us to determine the approximate size of the structure. The PTE was detected by all three s/c within some 30 s, even though the s/c were separated by up to 600 km. This implies that the relative velocity of the PTE in Fig. 10 is greater than 20 km/s, an order of magnitude larger than the speed of the s/c at these heights. The lower limit of the width is then determined by the s/c motion. Considering the ≈2 min traversal time of the PTE in Fig. 10, we obtain an estimate of the minimum width of the structure in the XY-plane of about 200 km. The flow velocity in the XY-plane, varying between ±10 km/s (as determined by the ion drift), gives error bars in the range ±1000 km, i.e. much larger than the minimum size. A third way to determine the PTE width is to use remote-sensing by energetic particles. Traversing a flux tube of ion flux, depletion results in a bipolar gradient signature similar to that of a shear flow. Indeed, such a bipolar signature was observed in a more extended time period, during 2 February

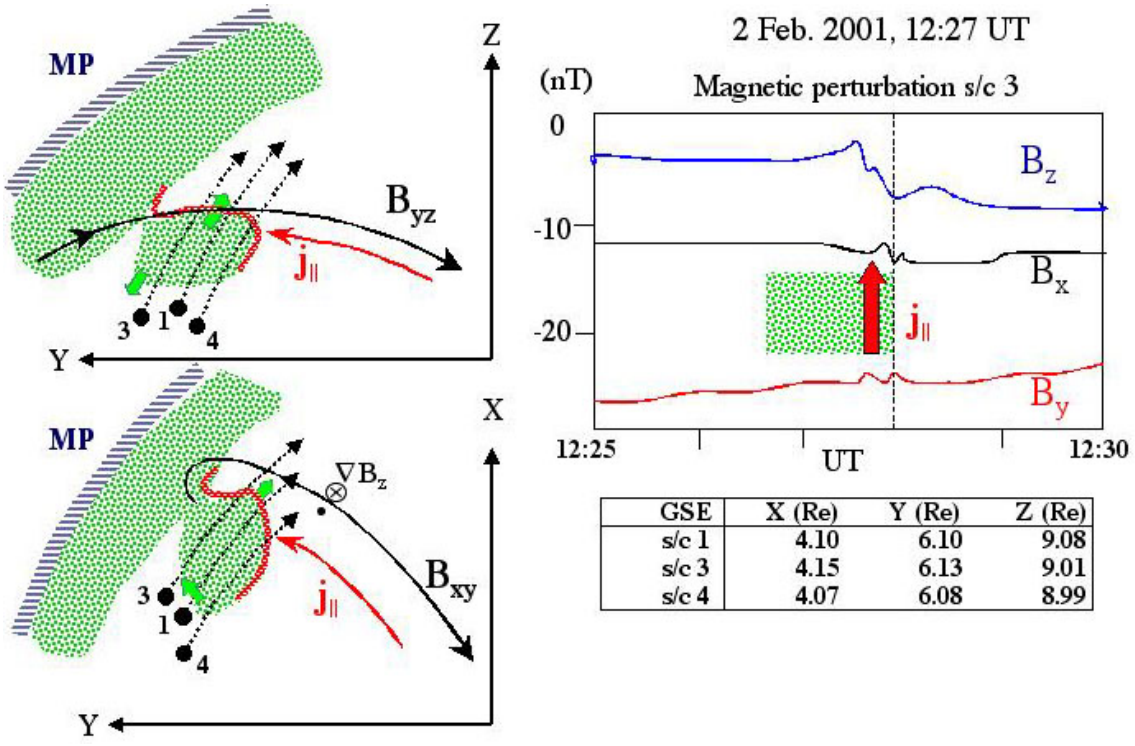

GSE	X (Re)	Y (Re)	Z (Re)
s/c 1	4.10	6.10	9.08
s/c 3	4.15	6.13	9.01
s/c 4	4.07	6.08	8.99

Fig. 10. Diagrammatic representation of the "stagnant" PTE on 2 February 2001, 12:27 UT.

2001, than that shown in Fig. 5. Taking 10 keV protons with Larmor radii of some 500 km in this event we find that the PTE was remotely sensed by energetic ions (>7 keV) for almost 20 min corresponding to 1200 km. If purely spatial, that implies a PTE width in the XY-plane of some 200±600 km.

As for the width in the Z-direction, the main direction of expansion, we note that the PTE centre expands with a velocity of ≈50 km/s downward and up to ≈100 km/s upward. Taking the 20 min. during which the PTE was observed with remote sensing, we obtain an extension in the Z-direction of ≈150 000 km (≈24 R_E), i.e. essentially filling the entire magnetic flux tube between the hemispheres. The Z-extension in Fig. 10, therefore, only marks a projection of the PTE in the s/c frame of reference.

Notice that the field-aligned current determined from the magnetic perturbations is again upward/antiparallel to B, connected to the sunward side of the PTE.

4 Discussion and conclusions

We have analyzed a set of Cluster observations of magnetosheath plasma transfer events, PTEs, through the dayside magnetopause, an analysis that leads to the following conclusions:

– PTEs are limited in space and time, characterized by magnetosheath plasma embedded in an environment of magnetospheric plasma.

– PTEs represent a class of observations highly variable in space and time, their properties varying significantly on Cluster spacecraft separation distances (January–April 2001).

– PTEs are found at high latitudes near local noon during most IMF conditions, albeit with a preference for IMF $B_z > 0$. The latter conclusion may be biased by the selection criteria, focusing as they did on cases when the spacecraft were in the dayside ring current/plasma sheet. During the analysis, we avoided cases of time-dependent magnetosheath plasma injection on clearly open magnetospheric field lines such as in the cusp. However, there are reasons to believe that temporal injection structures observed in the cusp are of a similar nature to those on closed field lines.

– PTEs have characteristics similar to those discussed in the impulsive penetration model (Lemaire, 1977; see also Echim and Lemaire, 2000, for a review). However, it remains to be understood why the occurrence of PTEs appears to be so independent of the IMF orientation. This is in contradiction to merging/reconnection (e.g. Cowley, 1982) and to some extent also with impulsive penetration.

– PTEs are generally associated with significant magnetic perturbations, indicating the presence of low-frequency wave activity and/or local currents. A bimodal magnetic signature, similar to that in a flux transfer event,

indicates that field-aligned currents couple to the sunward side of PTEs. The plasma drift near the sunward side also indicates a converging electric field there (converging $-\boldsymbol{v}\times\boldsymbol{B}$), implying that the upward field-aligned current connects to a negatively charged region, as expected if the current connects electrically to a voltage generator. To adequately understand the intrinsic properties of the PTE polarization and the related generation of currents would require a more thorough analysis involving Cluster electron and electric field data.

- PTEs near the magnetopause have a preference for antisunward motion, gradually shifting into more field-aligned motion further inside the magnetosphere yet maintaining a significant transverse ion drift. PTEs near the magnetopause for antiparallel magnetopause conditions, may be synonymous with FTEs (Russell and Elphic, 1979).
- Evanescent PTEs are structures lacking bulk flow, i.e. the plasma is not protruding further into the magnetosphere. Evanescent PTEs of "decaying" nature can be found quite deep inside the dayside ring current/plasma sheet.
- The injected/magnetosheath plasma may display fundamentally different dynamics compared to the ambient/magnetosphere ("cold" + hot) plasma in PTEs. Thus, the analysis of physical processes in a multicomponent boundary layer plasma is clearly not possible with traditional MHD. A multicomponent kinetic technique is required to determine the energy and mass transfer processes.
- PTEs, with the exception of completely evanescent PTEs, are associated with cross-field ion flow (ion drift). A difference in the ion drift for different plasma components may be observed, the injected magnetosheath plasma moving at a higher drift velocity compared to the "cold" background plasma (of H^+, He^+ and O^+). Cluster CIS data therefore corroborates previous findings from Prognoz-7 (e.g. Lundin and Dubinin, 1985; Lundin et al., 1987). This suggests that PTEs are associated with strong plasma gradients in time and/or space, a fact that stands out clearly when comparing data from different Cluster s/c. Gradients, with an order of magnitude ion flux drop within 1–2 Larmor radii, are not unusual (see e.g. Fig. 2).

Strong plasma pressure gradients are expected to generate electric fields and currents. The main sources of kinetic energy assumed to be available in PTEs for generating electromagnetic energy are the motional energy in the bulk flow and hydrostatic pressure gradients. From the electromagnetic dynamo equation

$$\boldsymbol{J}\times\boldsymbol{B}=\nabla\boldsymbol{P}_{\perp} \tag{3}$$

we note that a perpendicular pressure gradient ($\nabla\boldsymbol{P}_{\perp}$) may generate a current ($\boldsymbol{J}$) perpendicular to $\boldsymbol{B}$. The pressure gradient corresponds either to a plasma bulk flow perpendicular to B (flow/MHD dynamo) or to a hydrostatic pressure (thermoelectric generator), for instance:

$\nabla\boldsymbol{P}_{\perp}=$ $\nabla\boldsymbol{P}_K$ = kinetic pressure, corresponds to an MHD/flow dynamo and

$\nabla\boldsymbol{P}_{\perp}=$ $\nabla\boldsymbol{P}_H$ = static pressure, corresponds to a thermoelectric generator.

The analysis of PTEs indicates that both dynamo processes are relevant. Newly-injected PTEs have strong transverse bulk motion, a motion that gradually slows down leading to a kinetic pressure gradient opposite to the bulk flow. For evanescent PTEs with low bulk velocities of the injected plasma (e.g. 2 February 2001, Fig. 5), the inferred current is likely to be generated by residing static pressure gradients between injected and ambient magnetospheric plasmas. However, a more thorough analysis of local pressure conditions is required to understand the intrinsic dynamo properties.

As for the differential ion drift, a more detailed analysis is under way comparing, for instance, the drift for different ion species with EFW electric field data and making a detailed analysis of the differential drift to evaluate the contributions from kinetic and static pressure gradients. Already one may note that the observation of differential drift is in general agreement with earlier findings (Lundin and Dubinin, 1985) of the differential drift as the signature of a dynamo process.

An unloaded voltage generator is characterized by $\boldsymbol{E}+(\boldsymbol{v}\times\boldsymbol{B})=0$, i.e. the plasma is convecting without any dissipation/breaking. In a loaded dynamo kinetic energy is dissipated and a breaking force acts on the plasma. The plasma breaking can be described as an inertial force per unit volume $\boldsymbol{F}_i=\rho\,\mathrm{d}\boldsymbol{v}/\mathrm{dt}$, where ρ = nm is the plasma mass density. Neglecting all other possible sources for breaking (magnetic gradient drift, pressure, collision, etc.) the momentum equation can be written:

$$\rho\frac{d\boldsymbol{v}}{dt}=nq(\boldsymbol{E}+\boldsymbol{v}\times\boldsymbol{B}) \tag{4}$$

where n is the plasma number density and q is the electronic charge. Thus, whenever a force is acting, i.e. momentum is transferred, an imbalance occurs such that $\boldsymbol{E}+(\boldsymbol{v}\times\boldsymbol{B})=\boldsymbol{E}^*\neq 0$. A physical explanation for the departure from "ideal MHD" is that a loading of the dynamo introduces a depolarization current reducing the electric field in the plasma frame of reference such that $\boldsymbol{E}+(\boldsymbol{v}\times\boldsymbol{B})=<0$, i.e. $(\boldsymbol{v}\times\boldsymbol{B})>\boldsymbol{E}$. In this way a dynamo under load is characterised by a difference in drift velocity between the dynamo plasma and the local plasma. Plasma breaking may be associated with an external load (e.g. field-aligned currents coupled to the ionosphere) or an internal load (local mass loading by an ambient plasma). During internal loading (acceleration) the local plasma experiences an electric field:

$$\boldsymbol{E}=-(\boldsymbol{v}\times\boldsymbol{B})+\boldsymbol{E}^*$$

A local homogeneous plasma, initially at rest, will then drift with a speed less than the transverse speed of the dynamo plasma. Indeed, a frequent characteristic of PTEs is that the injected magnetosheath plasma drifts with a higher velocity than the "cold" local plasma (see Fig. 7), an observational characteristic noted already by Lundin and Dubinin (1985) although based on coarser and more sparsely-spaced data from Prognoz-7.

In summary, we conclude from the above Cluster observations that magnetosheath plasma protrudes into the dayside magnetopause near the cusp in a way similar to that described by the "impulsive penetration" model (Lemaire, 1977, see also a review by Echim and Lemaire, 2000). There are a number of characteristics in the PTEs that agree with an impulsive injection of plasma clouds into the magnetosphere governed not only by IMF properties but also by other characteristics in the magnetosheath such as the solar wind plasma pressure (Woch and Lundin, 1992; Stenuit et al., 2001). The PTEs are associated with magnetic perturbations, frequently with bimodal magnetic signatures very similar to those found in FTEs. The magnetic signature of PTEs is similar to that of FTEs, i.e. the magnetic perturbation corresponds to a field-aligned line current (Russell, 1984). The question is: are FTEs and PTEs just related or are they one and the same phenomenon – two sides of the same coin? Many characteristics point to the same mechanism for the two phenomena although FTEs are generally identified by the magnetic signature in the magnetosheath while PTEs are identified by the plasma signature in the magnetosphere. No doubt the access of magnetosheath plasma into the magnetosphere must be associated with an "opening", a hole in the magnetopause (Sonnerup, 1987). This leads to an outflow of magnetospheric plasma into the magnetosheath and an inflow of magnetosheath plasma into the magnetosphere. However, the main and distinguishing difference in interpretation is related with what happens next:

– Does the injection flux tube remain open for an extended time period, i.e. after merging of a magnetospheric flux tube with the magnetosheath, does the flux tube remain open and the plasma "frozen" into the flux tube? The flux tube may convect along a large-scale pattern until reconnecting with magnetospheric field lines much later (e.g. in the magnetotail).

– Is the opening/hole closed on a time scale considerably less than the time scale of large-scale convection and is the injected plasma effectively protruding faster than the electric drift? This implies that plasma is being transferred by motional forcing where the plasma drift is governed not only by the electric field but also by other forces that are equally large and individual for individual species and origin. A single flux tube concept is misleading under those circumstances.

The two interpretations differ in that one (the magnetic flux model) emphasises the transport and storage of potential energy (magnetic flux), while the other emphasises the local dissipation of plasma kinetic energy by electric currents.

The bimodal magnetic field signature of field-aligned currents, the observation of sharp plasma gradients and the dissipation of energy, as inferred from the ion differential drift in PTEs, all favor a local generation of electric fields and currents driven by plasma flow across magnetic field lines. The fact that PTEs are observed independently of the IMF makes them apparently different to FTEs. However, the IMF dependence found by e.g. Berchem and Russell (1984) is possibly enhanced by latitude effects, the ISEE satellites not reaching up to cusp latitudes. As was pointed out by e.g. Crooker (1980) and Staziewicz (1991), merging in the cusp may take place for a much broader range of IMF conditions. If so, and accepting that magnetic boundary conditions are decisive for plasma intrusion, one may argue that the lack of IMF dependence for the occurrence of PTEs is evidence for the cusp as the major region of solar wind plasma entry into the Earth's magnetosphere. This does not preclude plasma entry via FTEs near the subsolar point but only suggests that FTEs at the subsolar point are a special case of more frequent plasma injection near the cusp. Alternatively, plasma protrudes into the magnetopause and accesses the magnetosphere almost anywhere on the dayside magnetosphere, sustained by other conditions than classical merging. The relatively weak dependence of PTEs on IMF noted by Woch and Lundin (1992), even with a "reversed" dependence (favouring IMF $B_z > 0$) reported by Stenuit et al. (2001), may at first glance appear puzzling. Moreover, classical merging implies an increased entry of solar wind plasma into the magnetosphere for southward IMF and increased magnetospheric activity. However, as noted by Baumjohann et al. (1989) and Lennartsson (1991) the plasma sheet accumulates solar wind plasma at a faster rate for northward IMF, indicating that solar wind plasma injection as such plays a limited role in the accumulation of magnetotail energy associated with substorms and magnetic storms. The plasma injection process is likely to be primarily associated with energy dissipation in the dayside, as evidenced by the persistency of dayside auroral activity, being much less dependent on the overall magnetospheric activity (e.g. Murphree et al., 1981; Evans et al., 1985; Meng and Lundin, 1986).

The direct cause of the penetration of magnetosheath plasma through the magnetopause remains open. We have already noted that the magnetic boundary conditions applicable for merging as well as impulsive penetration make the cusp and its environs more accessible for a wider range of IMF conditions which is a requirement according to the observations of PTEs. However, previous studies (e.g. Woch and Lundin, 1992; Newell and Meng, 1994; Stenuit et al., 2001) indicate a strong dynamic pressure dependence for the PTE frequency of occurrence. This suggests that local pressure variations at the magnetopause may be more relevant than traditional magnetic merging conditions. An intriguing hypothesis that may solve the above dilemmas has been presented by Song and Lysak (1994, 1997, 2000). The Song and Lysak "alfvenon" model combines the electro-

magnetic causal dependence of merging (wave aspect) and the dynamical aspect of impulsive penetration (particle aspect). Even more importantly, they address the dualism in physics between the field formalism and the particle formalism that Hannes Alfvén pointed out some 20 years ago (Alfvén, 1981), a dualism that still has a strong impact on space plasma physics. Song and Lysak have presented a very elegant solution to the dualistic problem, realising that the problem is not only local but also propagates to other regions by means of field-aligned currents. A more careful analysis combining Cluster fields and particle data with the Song and Lysak alfvenon model is an obvious task for the future.

Acknowledgements. This paper was completed while the main author (R. Lundin) was enjoying a stay as visiting scientist at CESR/CNRS in Toulouse February – June 2001. The support from the CNRS was an essential ingredient in the success of this work. I am also indepted to the staff at CESR for their professional and invaluable support during a very productive visit. Special thanks to Dominique LeQueau, director of CESR, for organizing the visit and last but not least Hélène Perrier for assistance with the many practicalities. The Cluster project was managed and funded by the European Space Agency. The French part of Cluster CIS was funded by CNES and CNRS while the Swedish contribution was funded in part by the Swedish National Space Board and the Wallenberg Foundation.

Topical Editor G. Chanteur thanks two referees for their help in evaluating this paper.

References

Alfvén, H.: Cosmic plasma, D. Reidel Publishing company, Dordrecht, 1981.

Balogh, A., Dunlop, M. W., and Cowley, S. W. H.: The Cluster magnetic field investigation, Space Science Reviews, 79, 65–91, 1997.

Baumjohann, W., Paschmann, G., and Catell, C. A.: Average plasma properties in the central plasma sheet, J. Geophys. Res., 94, 6597–6606, 1989.

Berchem, J. and Russell, C. T.: Flux transfer events on the magnetopause: Spatial distribution and controlling factors, J. Geophys. Res., 89, 6689f, 1984.

Bostick, W. H.: Experimental study of ionized matter projected across a magnetic field, Phys. Rev., 104, 292–298, 1956.

Carlson, C. W. and Torbert, R. B.: Solar wind ion injections in the morning auroral oval, J. Geophys. Res., 85, 2903f, 1980.

Cowley, S. W. H.: The causes of convection in the Earth's magnetosphere – A review of developments during the IMS, Rev. Geophys. Space Phys., 20, 531–565, 1982.

Crooker, N. U.: The half-wave rectifier response of the magnetosphere and antiparallel merging, J. Geophys. Res., 85, 575–578, 1980.

Echim, M. M. and Lemaire, J. F.: Laboratory and numerical simulations of the impulsive penetration mechanism, Space Sci. Rev., 92, 565–601, 2000.

Evans, D. S.: The characteristics of a persistent auroral arc at high latitude in the 1400 MLT sector, The Polar Cusp, (Eds) Holtet, J. A. and Egeland, A., D. Reidel Publ. Comp., 99–109, 1985.

Heikkila, W. J.: Impulsive plasma transport through magnetopause, Geophys. Res. Lett., 9, 159–162, 1982.

Lennartson, W.: Solar control of the Earth's emission of energetic O^+, J. Atm. and Terr. Phys., 53, 1103–1111, 1991.

Lennartsson, W.: Statistical investigation of IMF B_z effects on energetic (0.1–16 keV) magnetospheric O^+ ions, J. Geophys. Res., 100, 23 621–23 636, 1995.

Lemaire, J.: Impulsive penetration of filamentary plasma elements into the magnetospheres of the Earth and Jupiter, Planet Space Sci., 25, 887–890, 1977.

Lemaire, J. and Roth, M.: Penetration of solar wind plasma elements into the magnetosphere, J. Atmos. Terr. Phys., 40, 331–335, 1978.

Livesey, W. A. and Pritchett, P. L.: Two-dimensional simulations of a charge-neutral plasma beam injected into a transverse magnetic field, Phys. Fluids B, 1, 914–922, 1989.

Lockwood, M. and Smith, M. F.: The variation of reconnection rate at the dayside magnetopause and cusp ion precipitation, J. Geophys. Res., 97, 14 841–14 847, 1992.

Lundin, R. and Dubinin, E.: Solar wind energy transfer regions inside the dayside magnetopause – I. Evidence for magnetosheath plasma penetration, Planet. Space Sci., 32, 745–755, 1984.

Lundin, R. and Dubinin, E.: Solar wind energy transfer regions inside the dayside magnetopause – II. Accelerated hevy ions as tracers for MHD-processes in the dayside boundary layer, Planet. Space Sci., 33, 891–907, 1985.

Lundin, R., Stasiewicz, K., and Hultqvist, B.: On the interpretation of different flow vectors of different ion species in the magnetospheric boundary layer, J. Geophys. Res., 92, 3214–3222, 1987.

Lundin, R.: On the magnetospheric boundary layer and solar wind energy transfer into the magnetosphere, Space Sci. Rev., 48, 263–320, 1989.

Ma, Z. W., Hawkins, J. G., and Lee, L. C.: A simulation of impulsive penetration of solar wind irregularities into the magnetosphere at the dayside magnetopause, J. Geophys. Res., 96, 15 751–15 765, 1991.

Meng, D.-I. and Lundin, R.: Auroral morphology of the midday oval, J. Geophys. Res., 91, 1572–1584, 1986.

Murphree, J. S., Cogger, L. L., Anger, C. D., et al.: Characteristics of the instantaneous auroral oval in the 1200–1800 MLT sector, J. Geophys. Res., 86, 1981–1992, 1981.

Newell P. T. and Meng, C.-I.: The cusp and the cleft/LLBL: Low-altitude identification and statistical local time variation, J. Geophys. Res., 93, 14 549–14 556, 1988.

Newell, P. T. and Meng, C.-I.: Ionospheric projection of magnetospheric regions under low and high solar wind pressure conditions, J. Geophys. Res., 99, 273–286, 1994.

Owen, C. J. and Cowley, S. W. H.: "Heikkilas" mechanisms for impulsive plasma transport through the magnetopause: A reexamination, J. Geophys. Res., 96, 5565–5574, 1991.

Phan, T.-D. and Paschman, G.: Low-latitude dayside magnetopause and boundary layer for high magnetic shear, J. Geophys. Res., 101, 7801–7816, 1996.

Rème, H., Aoustin, C., Bosqued, J. M., Dandouras, I., et al.: First multispacecraft ion measurements in and near the Earth's magnetosphere with the identical Cluster ion spectrometry (CIS) experiment, Ann. Geophys., 19, 1303–1354, 2001.

Riedler, W., Torkar, K., Rüdenauer, F., et al.: Active spacecraft potential control, Space Science Reviews, 79, 271–302, 1997.

Russell, C. T. and Elphic, R. C.: ISEE observations of flux transfer events at the dayside magnetopause, Geophys. Res. Lett., 6, 33–36, 1979.

Russell, C. T.: Magnetic reconnection in space and laboratory plasmas, (Ed) Hones, E. W., AGU monograph, p 124, 1984.

Sauvaud, J.-A., Lundin, R., Rème, H., et al.: Intermittent thermal plasma acceleration linked to sporadic motions of the magnetopause, first Cluster results, Ann. Geophysicae, 19, 1523–1532, 2001.

Schindler, K.: On the role of irregularities in plasma entry into the magnetosphere, J. Geophys. Res, 84, 7527–7266, 1979.

Schmidt, G.: Motion of plasma across magnetic field lines, Phys. Fluids., 3, 961–965, 1960.

Smith, M. F. and Lockwood, M.: The pulsating cusp, Geophys. Res. Lett., 17, 1069–1072, 1990.

Sonnerup, B. U. Ö.: On the stress balance in flux transfer events, J. Geophys. Res., 92, 8613–8625, 1987.

Song, Y. and Lysak, R. L.: "Alfvenon", driven reconnection and the direct generation of the field aligned currents, Geophys. Res. Lett., 21, 1755–1758, 1994.

Song, Y. and Lysak, R. L.: Some theoretical aspects of the solar wind-magnetosphereic interaction, Phys. Chem. Earth, 22, 715–721, 1997.

Song, Y. and Lysak, R. L.: Paradigm transition in cosmic plasma physics: Magnetic reconnection and the generation of field-aligned currents, Magnetospheric Current System, AGU Monograph, 2000.

Stasiewicz, K.: A global model of gyroviscous field line merging at the magnetopause, J. Geophys. Res., 96, 77–86, 1991.

Stenuit, H., Sauvaud, J.-A., Delcourt, D. C., Mukai, T., Kokobun, S., Fujimoto, T., Buzulukova, N. Yu., Kovrazhkin, R. A., Lin, R. P., and Lepping, R. P.: A study of ion injections at the dawn and dusk polar edges of the auroral oval, J. Geophys. Res., 106, 29 619–29 632, 2001.

Woch, J. and Lundin, R.: Temporal magnetosheath plasma injection observed with Viking: A case study, Ann. Geophysicae, 9, 133–142, 1991.

Woch, J. and Lundin, R.: Signatures of transient boundary layer processes observed with Viking, J. Geophys. Res., 1431–1447, 1992.

Yamauchi, M., Woch, J., Lundin, R., Shapshak, M., and Elphinstone, R.: A new type of ion injection event observed by Viking, Geophys. Res. Lett., 20, 795–798, 1993.